The Nature of O_2 Reactivity Leading to Topa Quinone in the Copper Amine Oxidase from *Hansenula polymorpha* and Its Relationship to Catalytic Turnover†

Jennifer L. DuBois§ and Judith P. Klinman*

Department of Chemistry and Department of Molecular and Cell Biology, University of California at Berkeley, Berkeley, California 94720

Received March 14, 2005; Revised Manuscript Received May 25, 2005

ABSTRACT: The copper amine oxidases (CAOs) catalyze the O_2-dependent, two-electron oxidation of amines to aldehydes at an active site that contains Cu(II) and topaquinone (TPQ) cofactor. TPQ arises from the autocatalytic, post-translational oxidation of a tyrosine side chain in the active site. Monooxygenation within the ring of tyrosine at a single Cu(II) site is unique in biology and occurs as an early step in the formation of TPQ. The mechanism of this reaction has been further examined in the CAO from *Hansenula polymorpha* (HPAO). When a Clark electrode fitted to a custom-made, gastight apparatus over a range of initial concentrations of O_2 was used, rates of O_2 consumption at levels greater than air are seen to be reduced relative to earlier results, yielding K_D(apparent) = 216 μM for O_2. This is consistent with a mechanism in which O_2 binds reversibly to the active site, triggering a conformational change that promotes ligation of tyrosinate to Cu(II). The activated Cu(II)-tyrosinate species has been proposed to react with O_2 in a rate-limiting step, although it was also possible that breakdown of a putative peroxy-intermediate controlled TPQ formation. To test the latter hypothesis, Cu(II)-free HPAO was prepared with 3,5-ring-[$^2H_2$]-tyrosine incorporated throughout the primary sequence. The absence of an isotope effect on the rate of TPQ formation eliminates cleavage of this C−H bond in a proposed Cu(II)-aryl-peroxide intermediate as a rate limiting step. The role of methionine 634, previously found to moderate O_2 binding during the catalytic cycle, is shown here to serve a similar function in TPQ formation. As with catalysis, the rate of TPQ formation correlates with the volume of the hydrophobic side chain at position 634, implicating similar binding sites for O_2 during catalysis and cofactor biogenesis.

The copper amine oxidases (CAOs)[1] are unusual in their facilitation of completely separate, O_2-dependent reactions. As catalysts, the CAOs carry out the two-electron oxidation of amines to aldehydes, yielding H_2O_2 as a byproduct (Scheme 1) (*1*). However, before catalysis can occur, the enzyme must first form its cofactor via a monooxygenation, hydration, and two-electron oxidation of tyrosine to yield 2,4,5-trihydroxyphenylalanine quinone (topaquinone or TPQ). This reaction is solely dependent on the active site Cu(II) and O_2, and occurs in vitro without the assistance of added cofactors or proteins(*2*−*4*).

The TPQ formation reaction involves an initial monooxygenase reaction at an active site containing a single Cu(II) ion, in the absence of reducing equivalents for activating O_2. As a result of extensive investigations, a substrate-activation mechanism has been proposed (Scheme 2) (*4*). According to this mechanism, a precursor tyrosinate (Tyr405 in the enzyme from *Hansenula polymorpha*, HPAO) binds Cu(II), forming a Cu(II)−tyrosinate species with a small degree of Cu(I)-tyrosyl resonance stabilization (Scheme 2). This Cu(II)-tyrosinate has been tentatively identified as the O_2-dependent absorbing species (λ_{max} = 350 nm) previously seen when the cofactor formation process is monitored optically (*5*). Because this species only forms in the presence of O_2, it has been proposed that O_2 binding in the active site promotes a conformational change that leads to ligation of Tyr405 to Cu(II). Decay of the intermediate's absorbance is associated through an isosbestic point with cofactor formation (TPQ λ_{max} = 480 nm), indicating that breakdown of this intermediate is a rate-determining step in the overall reaction. Though the proposed mechanism of biogenesis is consistent with the available experimental data (*5*−*7*), there are a number of unanswered questions about the O_2-dependent steps. For example, is it possible that a species other than a

Scheme 1: Catalysis of Amines by CAOs[a]

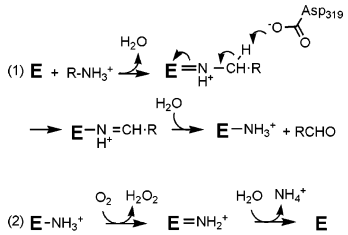

[a] (1) reductive half reaction; (2) oxidative half reaction.

† This work was supported by National Institutes of Health Grants (GM 39296 and GM 25765). J.L.D. was supported by a National Institutes of Health Post-Doctoral Fellowship (GM 63414−01).

* To whom correspondence should be addressed. Phone: (510) 642-2668. Fax: (510) 643-6232. E-mail: klinman@berkeley.edu.

§ Present address: Department of Chemistry and Biochemistry, University of Notre Dame, Notre Dame, IN 46556.

[1] Abbreviations: CAO, copper amine oxidase; TPQ, 2,4,5-trihydroxyphenylalanine quinone; HPAO, copper amine oxidase from *Hansenula polymorpha*; WT- HPAO, wild-type HPAO; E, enzyme; RLS, rate-limiting step; IPTG, isopropylthio-β-D-galactoside.

10.1021/bi0504759 CCC: $30.25
Published on Web 08/04/2005

Scheme 2: Proposed Cofactor Formation Mechanism[a]

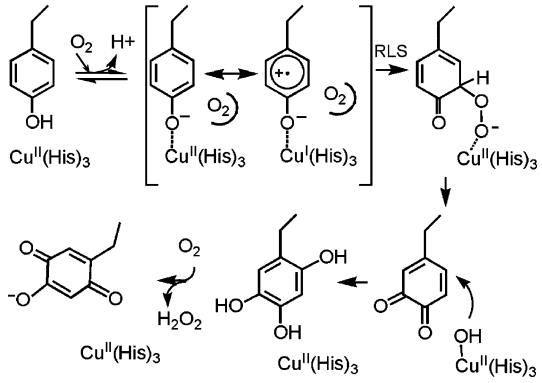

[a] As Cu(I)−tyrosyl has never been observed, this extreme resonance form must be present at very low concentration.

Cu(II)−tyrosinate is the source of the observed 350 nm absorbance? Additionally, what is the position of O_2 binding during biogenesis and how is this linked to the absorbance changes?

To obtain greater mechanistic detail for the reaction of the precursor protein with O_2, its single turnover kinetics were previously studied as a function of [O_2] (*6, 7*). Because the reaction with O_2 is slow ($t_{1/2}$ = 14 min, pH 7, 25 °C) and consumes only 2 equiv of O_2 (*8*), it is difficult to measure O_2 depletion reliably with the standard Clark-type O_2 electrode (especially at elevated O_2 concentrations). A new, rigorously gastight chamber was therefore designed, with needle-access to the reaction space, temperature control, no headspace gas, and constant stir speeds over the time course measured. These modifications have allowed for more accurate measurements of O_2 consumption rates during cofactor formation over the range of O_2 concentrations considered, leading to an estimate of K_D(apparent) = 216 μM for O_2.

Deuteration at the ring-3,5 positions of Tyr405 has also been studied to probe its effect on the rate of cofactor formation and to place further limits on the proposed rate-determining step. Finally, a residue previously identified as critical to O_2 chemistry during catalytic turnover in HPAO (*9*) has been assessed for its role in the O_2 chemistry of TPQ formation. This residue, methionine 634, appears to have a similar function in O_2 binding during TPQ formation and catalysis and may be part of the conformational switch that leads to the critical Cu(II)−tyrosinate complex.

EXPERIMENTAL PROCEDURES

Mutagenesis, Protein Expression, and Purification. All chemicals were of the highest available grade of purity and used without further purification. The wild-type HPAO gene (WT-HPAO) was previously subcloned into a pET3a expresssion vector (Stratagene) (*10*). Mutagenesis of HPAO was carried out using a QuickChange kit (Stratagene). Primers used (mutated codons underlined) were 5′-CCTGAGGACTTCCCATTGGCCCCGGCCGAGCCTATCACC-3′ (M634A); 5′- CCTGAGGACTTCCCATTGTTCCCGGCCGAGCCTATCACC-3′ (M634F); 5′- CCTGAGGACTTCCCATTGCTGCCGGCCGAGCCTATCACC-3′ (M634L). Plasmids were transformed into electroporation-competent BL21(DE3) cells (Stratagene) for expression and storage (in 40% glycerol, −80 °C).

Growth of BL21(DE3) cells for protein expression followed previously described procedures (*3*), with some modifications. A single colony was picked from a freshly streaked plate (LB-agar, supplemented with 0.1 mg/L ampicillin) after ∼10 h of incubation at 37 °C and inoculated into 400 mL metal-free growth medium (50% M9 salts, 50% 20 mg/L casein, where the casein has been stirred at least 45 min with 15 g/L of the metal chelating resin, Chelex 100, Sigma). Growth medium was supplemented with 0.1 mg/L sterile, filtered ampicillin and $MgSO_4$/dextrose (to a final concentration of 0.6 mM $MgSO_4$, 4 g/L dextrose). The 400 mL culture was grown on a shaker incubator overnight at 37 °C, 250 rpm. A volume of 30 mL of the overnight culture was inoculated into each of 12 flasks containing 1.5 L of growth medium. Flask cultures were grown on a shaker (37 °C, 250 rpm) for ∼3 h until the cells reached an absorbance at 600 nm of 0.5−0.6. Cells were induced by addition of 1 mM IPTG and grown for 4 h before collection by centrifugation. Cell pellets were disrupted immediately by sonication, and the soluble portion was collected by centrifugation. Dialysis, ion exchange, and gel filtration column purification steps were carried out as previously described (*3*). Pure fractions were pooled and concentrated to ∼1.5 mL in a centrifuge filter with a 10 000 molecular weight cut off (Millipore). Pure protein was exchanged into 50 mM HEPES buffer, pH 8, by three cycles of concentration and resuspension in 5−10 vol of this buffer.

WT-HPAO was overexpressed in the presence of ring-3,5-[$^2H_2$]-tyrosine to obtain enzyme incorporating the deuterated tyrosine. Cells were grown in a defined amino acid medium lacking tyrosine (in place of casein, 0.14 g/L each of the remaining amino acids supplemented by 10 mL/L of sterile BME vitamin solution (Sigma), stirred at least 45 min with 15 mg/L with the metal-chelating resin Chelex 100, (Sigma)). Labeled tyrosine (Cambridge Isotopes) was added to a final concentration of 220 mg/L at the time of induction. Protein was purified as described above.

Protein Characterization Methods. Protein concentrations were measured by the Bradford assay with bovine serum albumin as a standard (Bio-Rad Laboratories). Per-subunit Cu concentrations of metal-reconstituted proteins were measured by inductively coupled plasma atomic emission spectrometry (ICP-AES, Optima 3000 DV from Perkin-Elmer), after eliminating unbound Cu(II) from the samples by buffer exchange (three cycles of dilution in 3−5 vol of metal-free 50 mM HEPES, followed by concentration in a centrifuge microconcentrator, 10 000 molecular weight cut off, Millipore). The degree of ring-3,5-[$^2H_2$]-tyrosine incorporation into labeled protein was determined by quantitative liquid chromatography/tandem mass spectrometry (LC-MS/MS) on a Micromass Q-Tof hybrid quadrupole-time-of-flight mass spectrometer, carried out by the Stanford PAN facility. Proteins (1−2 mg) were reduced, and the cysteines iodoacetylated. Proteins were then segmented into <4000 molecular weight peptides by proteolysis using trypsin (2 mg, 8 M urea, 37 °C, 24 h). Masses of six randomly selected tyrosine-containing peptides were determined by LC-MS/MS as a measure of the extent of label incorporation into the protein as a whole.

Cofactor Formation Kinetics. TPQ formation was monitored spectrophotometrically on an HP8452A (Hewlett-Packard) UV−visible spectrophotometer fitted to a temper-

Scheme 3: Modified Clark Electrode for Measurement of O_2 Uptake under Gastight Conditions[a]

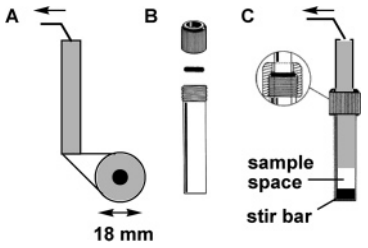

[a] (A) Teflon housing for microelectrode, with arrow indicating electronic input to O_2 monitor; (B) gastight glass measurement chamber, derived from ChemThread (ChemGlass) tubing with compression cap and viton O-ring; (C) complete assembly of Teflon-housed electrode in glass measurement chamber, with laminar stir bar. The complete assembly fits into a plexiglass temperature control chamber linked to a circulating water bath and rests on a digitally controlled stir plate. (B) and (C) are adapted from the ChemGlass catalog.

ature control bath. A quartz cuvette with a 100 μL fill volume was fused to a small tear drop flask with a standard 14/20, septum-sealable neck. This was used with 94−96 μL samples containing 40−60 μM apoprotein monomer (HPAO is a homodimer) in 50 mM HEPES buffer, pH 8. Samples were spread over the surface of the flask portion of the septum-sealed cuvette and made anaerobic by a continuous purge of argon for 20−30 min at 4 °C. A 1 mM solution of $CuCl_2$ was similarly made anaerobic by continuous bubbling of argon for 20−30 min. One equivalent of Cu(II) was added by gastight syringe to the protein samples, and changes in the spectrum (200−700 nm) were monitored every 1−2 min for 1 h. Once the spectrum stopped changing, a t_0 spectrum was measured and the samples were opened and purged with air from a compressed air line for 10−15 s. Spectra were measured at 2- or 10-minute intervals for 1−12 h (i.e., for a duration at least 3 times the formation $t_{1/2}$ of the WT or mutant sample) under conditions of 25 °C. Changes at λ_{max} = 480 nm for TPQ were fitted to single-exponential curves of the form $y = m_1(1 - e^{-kx}) + m_2$, using the KaleidaGraph program, to determine the characteristic k_{obs}.

O_2 Electrode Construction. An O_2-sensitive electrode was purchased from Yellow Springs Instruments and used unmodified with the accompanying voltage converter box. The reaction chamber and cooling unit were designed and custom built as follows (cf., Scheme 3). A size 18 (22 mm outer diameter) threaded glass tube, with viton O-ring and Celcon compression cap (ChemGlass), was sealed with a flattened glass bottom to a total length of 8.5 cm. A resin-coated, disk-shaped, magnetic stirbar was cut and polished to fit the dimensions of the reaction chamber. A cylindrical Teflon housing for the electrode (length = 7.5 cm) was machined to fit snuggly into the interior of the glass tube. A threaded hole was bored out of the center of the housing to accommodate the electrode, followed by a Teflon screw used to secure the electrode in place. A 2 mm × 2 mm notch was cut down the length of the housing for needle access to the reaction space. This notch was widened to 5 mm near the top of the tube to fit a machined Teflon stopper used to close off the needle hole.

A temperature-control unit was constructed to fit the glass reaction chamber. A 6 cm tall piece of 7.5 cm inner diameter plexiglass tubing was cut and fitted with a plexiglass top and bottom. A bevelled hole was cut in the top of the unit to accommodate the reaction chamber. A viton O-ring and an aluminum plate with a hole cut to match the reaction chamber diameter were placed over the top of the unit, and the reaction chamber was inserted. Two holes in the aluminum plate were cut to match two screws. Tightening bolts on the screws crushed the O-ring and secured the reaction chamber tightly in place. The temperature-control unit was attached by tubing to a circulating, adjustable temperature water bath. The tubing was routed such that water flow diverted back to the bath when the temperature-control unit was opened, making it possible to keep the water bath circulating continuously when the reaction chamber was removed from the bath between measurements. The entire unit was placed on an IKA-RCT stir plate (VWR), and measurements were carried out under digitally monitored, constant stir rates.

O_2 Electrode Measurements. All work was carried out at 25.0 °C. The electrode was equilibrated and the voltage converter calibrated to a standard [O_2] before use: 2 mL of dH_2O were added to the chamber and stirred for 5 min to equilibrate under either air or a constant stream of pure O_2, added via a needle inserted into the needle slot and positioned just over the liquid surface. For measurements made at [O_2] ≤ 258 μM, the electrode was equilibrated to air and calibrated so that the full scale ($1V$) = 258 μM O_2. For measurements ≥ 258 μM, the electrode was equilibrated to pure O_2 and calibrated to $1V$ = 1170 μM O_2.

Two milliliters solutions of apo-WT-HPAO were similarly equilibrated to air, pure O_2, or a selected concentration of O_2 prepared by mixing a steady stream of N_2/O_2 gases, regulated from a pair of gas flow meters. Once equilibrated, the electrode position was adjusted to meet the liquid surface, excluding all bubbles and gaseous headspace in the process, and the crush cap was tightened. The reactions were stirred at constant speed, and a linear background rate was measured on a chart recorder. Given the stoichiometry of two molecules of O_2 consumed per TPQ formed (*8*), the observation that ∼30% of the apoprotein WT-HPAO forms TPQ after reconstitution with Cu(II), and absolute limitations imposed by the tendency of stirred protein to precipitate at higher concentrations, 2 mL samples, 20−50 μM in apoenzyme monomer (1.5−3.8 mg/mL), were employed. The chart recorder was adjusted to measure 5% of the calibrated full scale when calibrated to pure O_2 (63.5 μM) and 5−10% when calibrated to air (12.9−25.8 μM). This is 5−10 times the value of the expected system stability over 15 min and hence at least 5 times the minimal $\Delta[O_2]/\Delta t$ over which the electrode can be expected to give a linear response, as per manufacturer specifications (*13*). These values were chosen so that measured signals would exceed background rates determined at various concentrations of O_2 (see Results) for the duration of the measurement.

Once equilibrated, reactions were initiated by addition of 1 equiv of cupric chloride, injected via syringe from a 20 mM stock. After injecting, the needle port was sealed with a Teflon stopper and the measurement recorded for 30−90 min. Points were noted at 1-minute intervals and transferred to Microsoft Excel spreadsheets. Data were fit by curves of the form $y = m_1(e^{-kx}) + (m_2)x + m_3$ using the KaleidaGraph program, to account simultaneously for the single-exponential rate of O_2 depletion (with the associated $k(O_2)$) and the linear background rate. Background rates, measured before the

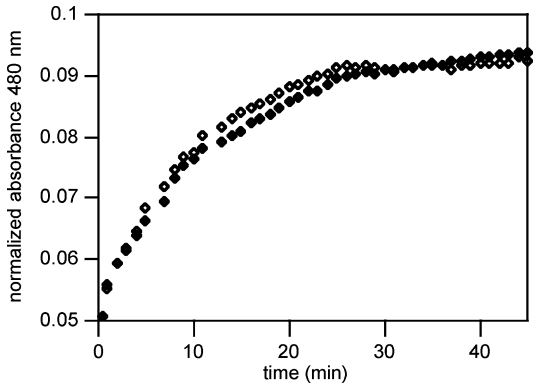

FIGURE 1: Appearance of the TPQ-associated 480 nm absorbance over time after oxygenation of Cu(II)-reconstituted apo-HPAO, perproteo HPAO (◇); HPAO-containing ring-3,5-[$^2H_2$]-tyrosine (◆). Single exponential curves fit to the data yield nearly identical values for $k_{(TPQ)}$, indicating the absence of a deuterium isotope effect.

reaction was initiated, were fit by linear regression and their slopes compared to background rates measured after completion of the measurement (m_2 above) to ensure O_2 consumption had returned to baseline levels.

The large amount of enzyme needed for individual measurements necessitated measuring data from multiple enzyme preparations. To minimize variation between batches, $k(O_2)$ data from each preparation were normalized according to the value of k_{TPQ} measured for the same preparation under a well-characterized set of standard conditions (pH 7, 25 °C, and 258 μM O_2). Briefly, the average of at least three values for k_{TPQ} measured for each preparation ($k_{average}$) was determined (data not shown). Values for $k_{average}$ were typically within 1−2 times the previously measured error range of 0.03 for the average value of k_{TPQ} (0.08 min^{-1}) (*5*). Measured values for $k(O_2)$ were adjusted by a factor of $k_{average}/k_{TPQ}$ obtained for each enzyme preparation. The same procedure was used previously in constructing the k_{TPQ} versus $[O_2]$ curve reproduced in Figure 3 (*6*).

RESULTS

Tyrosine 405 Ring-3,5-Deuterium Isotope Effect. Incorporation of ring-3,5-[$^2H_2$]-tyrosine into HPAO was assessed by quantitative LC-MS of a random selection of tyrosine-containing peptides from a tryptic digest. For each of six peptides measured, >99% were found to be mass-shifted by 2 units per tyrosine, relative to the theoretically predicted mass, indicating effectively stoichiometric incorporation of the labeled amino acid. TPQ formation was measured by monitoring absorbance changes at 480 nm over time (Figure 1). Single-exponential fits to the curves gave an average of three measurements, $k_{(TPQ)} = 0.10 \pm 0.02$ min^{-1} at pH 8. This is similar to the wild-type value of $k_{(TPQ)} = 0.08 \pm 0.03$ min^{-1} determined previously at pH 7. (*5*).

The Rate Constant for O_2 Consumption k*(O_2) during Biogenesis, as a Function of [O_2]*. Background rates of O_2 consumption for the newly constructed chamber (Scheme 3) were measured in buffer as a function of initial $[O_2]$ and found to be linear over at least 20 min. The rate of background O_2 consumption increased linearly with the initial $[O_2]$. Average rates of background O_2 consumption from air-saturated water were 0.3 μM/min (±0.1) and 1.1 μM/min (±0.4) from O_2-saturated water. These values are close to

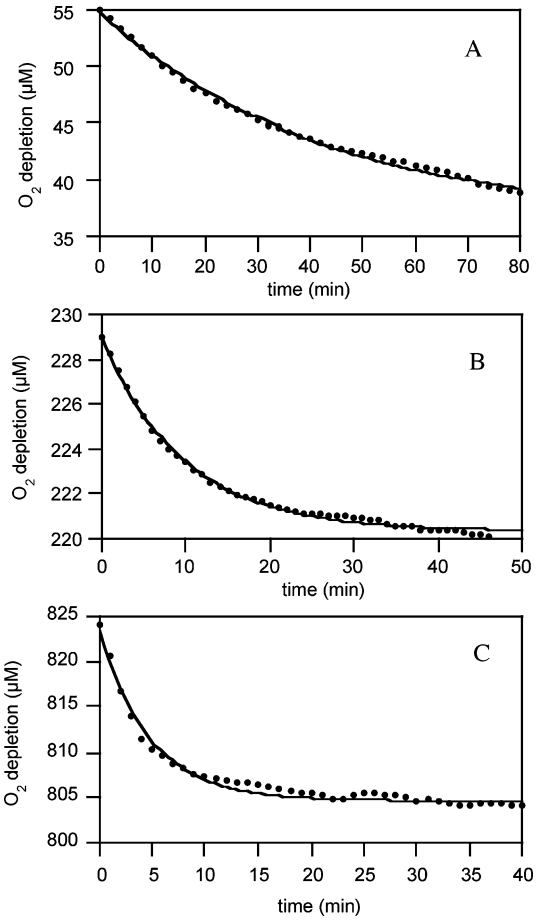

FIGURE 2: Representative kinetic traces following O_2 consumption during TPQ formation at (A) low (55 μM), (B) medium (229 μM), and (C) high (824 μM) initial values of $[O_2]$ within the measured range, using a Clark electrode in an airtight chamber.

the manufacturer's expected limits on electrode stability and linearity: ~1% of the full scale over 15 min (0.172 μM/min, air; 0.78 μM/min, pure $[O_2]$) (*11*). This corresponds to consumption of ~1.5 μM O_2 due to background over one TPQ formation half time (in air, 25 °C, 50 mM HEPES, pH 7) or ~7.5 μM over the duration of the measurement. To attain a reasonable signal-to-noise ratio, samples were made 30−40 μM in apoprotein. Higher concentrations resulted in rapid precipitation of protein upon Cu(II) addition. Background rates measured in the standard, unsealed reaction chamber were greater by an order of magnitude or more, were not linear beyond 5−10 min, and, when the $[O_2]$ was less than 258 μM (air saturated buffer), were opposite in slope due to O_2 entry into the chamber from atmosphere.

O_2 depletion during TPQ formation occurred with single-exponential decay kinetics (Figure 2). Values for $k(O_2)$ were obtained from curves measured for initial $[O_2]$ from 50 to 1100 μM. These, in turn, were plotted versus $[O_2]$ and fit to a hyperbolic curve, $y = m_1x/(x + m_2)$ (Figure 3). Here, m_2 is analogous to K_M from the Michaelis−Menten equation and represents a K_M(effective) = 216 (±45) μM for the single turnover process. The maximal value for $k(O_2)$ extrapolated from the curve is $k_{max} = 0.27$ (±0.021) min^{-1}. This is ~1.7 times faster than the extrapolated maximal rate of TPQ formation (0.16 ± 0.0083 min^{-1}, pH 7). The latter value was obtained by fitting a hyperbolic curve to a plot of $k_{(TPQ)}$ versus $[O_2]$, where $k_{(TPQ)}$ is the rate constant derived from

Table 1: Kinetic and Spectroscopic Characteristics of TPQ Formation in WT-HPAO and M634 Mutants

	WT	M634F	M634L	M634A
side-chain volume[a] (Å^3)	170	202	168	122
k_{TPQ} (min^{-1}) (in air, pH 8)	0.090 ± 0.03	0.11 ± 0.02	0.042 ± 0.01	0.0031 ± 0.0009
λ_{max} (nm) of mature cofactor	480	496	460	~480

[a] Numbers from ref *9*.

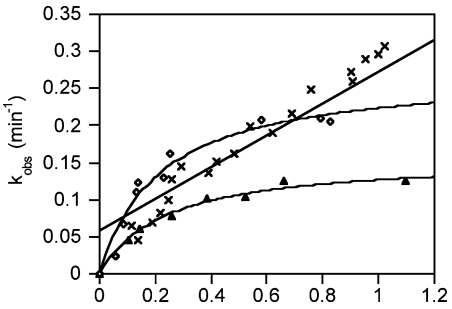

FIGURE 3: Rate constants for O_2 consumption during TPQ formation, and optically determined rate of TPQ formation, as a function of [O_2]. O_2 consumption data were measured by a Clark O_2 electrode in an unsealed (×) or sealed chamber (◇, this work). TPQ formation was measured by monitoring the TPQ 480 nm absorbance over time in 50 mM HEPES, pH 7 (▲); from ref *6*.

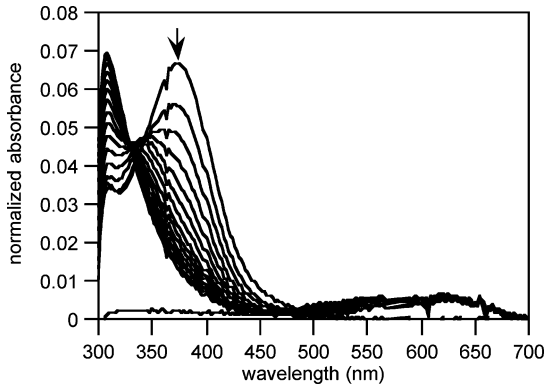

FIGURE 4: Spectral changes after anaerobic addition of Cu(II) to apo-M634F HPAO. Spectra shown were measured in 10-min intervals and are normalized to zero absorbance at 800 nm.

fitting a single-exponential curve to a plot of absorbance at 480 nm over time (*7*). The K_M(effective) measured under these conditions is 233 (±35) μM.

TPQ Formation and Spectroscopic Properties of M634 Mutants. TPQ formation was monitored spectrophotometrically in WT-HPAO and the M634 mutants, M634F, M634L, and M634A. These mutants were selected because all of the side chains are hydrophobic and because they span the range of side-chain volumes considered in a prior study of the catalytic properties of M634 mutants (Table 1) (*9*).

Samples of apoprotein were first made anaerobic, and 1 equiv of O_2-free Cu(II) was added via airtight syringe. In samples of WT, M634A, and M634L, a band at 380 nm appeared within the mixing time of the experiment and decayed to baseline with similar single-exponential kinetics in all cases (k(380 nm) ~ 0.65 min^{-1}). This band has been previously proposed to be due to a Cu-associated LMCT for copper bound outside of, but migrating into, the active site (*5*). In samples of M634F, uniquely, two bands appeared at 380 and ~600 nm (Figure 4). The 380 nm band decayed as with WT and the other mutants, while the 600 nm band appeared unchanged. Upon addition of O_2, the 600 nm band

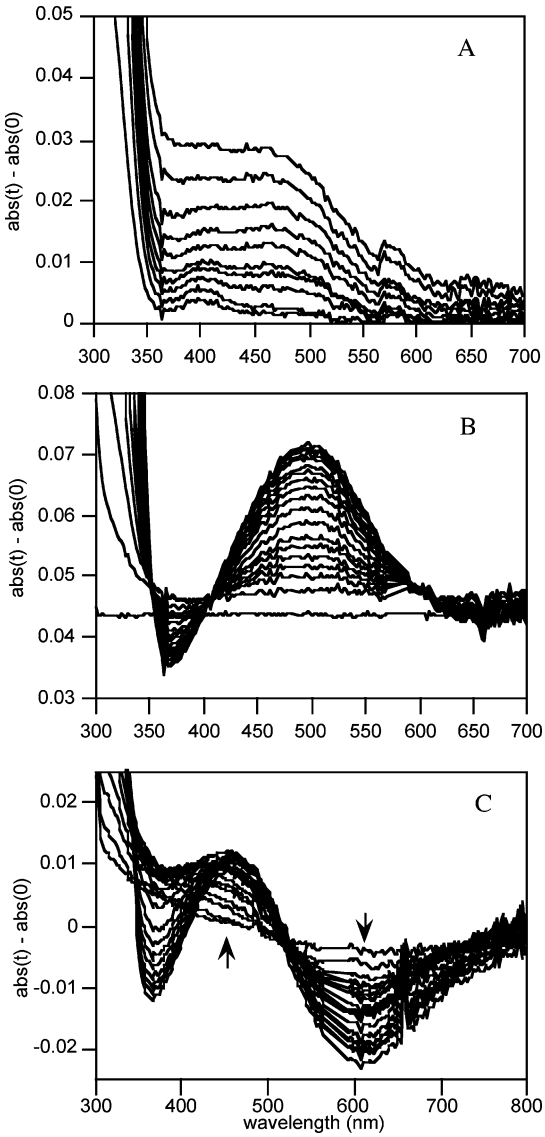

FIGURE 5: Spectral changes during TPQ formation in (A) M634A, (B) M634L, and (C) M634F. Samples are 60 μM in HPAO monomer. Cu(II) was added anaerobically to O_2-free samples of apoprotein, incubated for 90 min, and a baseline spectrum measured. O_2 was rapidly introduced into the reaction cuvette, and subsequent spectra were measured (A) once per hour, (B and C) every 2 min.

decayed with single-exponential kinetics as the TPQ associated band at 480 nm formed, with an isosbestic point between the two absorbances (Figure 5C). Because the 600 nm absorbance was unique to M634F and did not seem to interfere with TPQ formation, we did not explore it further. TPQ formed (pH 8) with $k_{(TPQ)} = 0.11 \pm 0.02$ min^{-1}. This rate constant is comparable to that measured for TPQ formation in WT-HPAO: $k_{(TPQ)} = 0.09 \pm 0.03$ min^{-1}. Smaller rate constants were measured for M634L (0.042 ± 0.01 min^{-1}) and M634A (0.0031 ± 0.0009 min^{-1}) (see Figure 5A,B). In a plot of $k_{(TPQ)}$ versus side-chain volume,

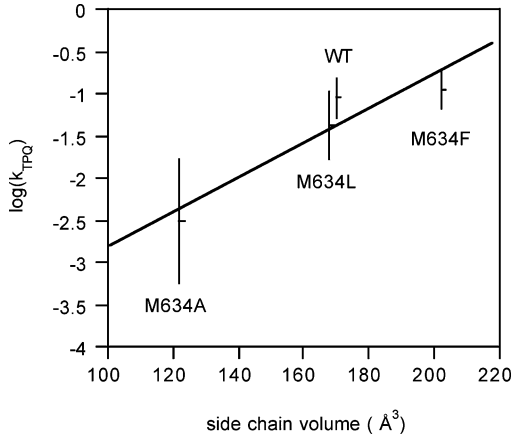

FIGURE 6: Relationship between $k_{(TPQ)}$ and side-chain volume for WT-HPAO and M634 mutants. Values for side-chain volumes are from ref *9*.

an approximately linear relationship was observed (Figure 6). This trend is similar to that previously observed for the kinetics of O_2 catalysis ($\log[k_{cat}/K_M(O_2)]$) by the mature enzyme (*9*).

DISCUSSION

Nature of the Rate-Determining Step in Biogenesis. The TPQ cofactor in CAOs forms via monooxygenation of the ring of an active site tyrosine followed by ring addition of water and a second, O_2-dependent oxidation (cf., Scheme 2). The goal of this study has been to understand how the enzyme facilitates this O_2-dependent chemistry as well as subsequent O_2-dependent oxidation of amines during catalytic turnover (Scheme 1).

Prior work showed that an O_2-dependent intermediate with $\lambda_{max} = 350$ nm appears upon addition of O_2 to the anaerobic, Cu(II)-bound precursor enzyme (E-Cu(II)-Tyr). The decay of this absorbance occurs isosbestically with the appearance of the TPQ absorbance at 480 nm. A model was put forth in which the intermediate is proposed to be a Cu(II)−tyrosinate ligand-to-metal charge transfer (LMCT) complex (*5*). This model accounts for the lack of a conventional metal-binding site for O_2 activation by postulating activation of the substrate tyrosine through a Cu(II)−tyrosyl resonance form of the LMCT complex. The proposed mechanism has several interesting implications that we sought to explore experimentally. First, formation of the intermediate must somehow depend on O_2. It was suggested that O_2 binding in the active site is linked to a conformational change, which promotes ligation of the tyrosine phenolate to Cu(II) (*5, 6*). An O_2-binding site associated with catalysis was previously identified using site-directed mutagenesis and kinetics measurements (*9, 12*). Similar approaches are used here to explore O_2 binding during TPQ biogenesis. Second, the decay of the 350 nm intermediate is expected to be a rate-determining step (*5*). Investigation of alternate, possible species as the origin of this intermediate was expected to narrow the choices for the actual structure.

If the intermediate is as proposed (a Cu(II)−tyrosinate), the rate-determining step would likely involve reaction of this species with O_2, either through one-electron transfer to O_2 or by a concerted two-electron process leading to formation of a Cu(II)−aryl-peroxide. In principle, these issues could be addressed directly by probing biogenesis for an $^{16}O_2/^{18}O_2$ isotope effect. However, because of the small amount of intermediate expected to accumulate and the single-turnover nature of the reaction (*5*), this approach is technically not feasible. We therefore sought to validate the proposed Cu(II)−tyrosinate intermediate and the consequent rate-limiting steps by ruling out the other chemically plausible intermediate: the Cu(II)−aryl-peroxide species predicted to form on reaction of the Cu(II)−phenolate/Cu(I)−phenoxyl with O_2 (Scheme 2). A Cu(II)−aryl-peroxide might also have a LMCT with the observed λ_{max} and ϵ values (*13*), such that cleavage of its C3−H bond would be the rate-determining step in cofactor production. The rate of TPQ formation was therefore measured in ring-3,5-[$^2H_2$]-tyrosine substituted protein and found to be identical to the rate measured for unsubstituted protein (Figure 1). The lack of any isotope effect on this C−H bond cleavage fails to support a Cu(II)−aryl-peroxide as the observed intermediate.

Identification of the O_2-Binding Site in Biogenesis. An important feature of the originally proposed Cu(II)−tyrosinate intermediate is a nonmetal-binding site for O_2, with O_2 binding causing the conformationally induced formation of the intermediate. Where could the O_2 bind? The crystal structure of Zn(II)-substituted HPAO, where Tyr405 remains unprocessed but is bound to Zn(II), has an active site that approximates the Cu(II)−tyrosinate structure (Figure 7A) (*14*). Two possible O_2-binding sites are apparent from this structure. First, O_2 could enter the active site via the substrate channel, binding next to the Tyr405 phenolic ring on the side nearest the active site base. Two water molecules, which could be displaced by O_2, occupy positions very close to the C5 and C6 ring carbons in the E-Zn(II)-Tyr crystal structure. Alternatively, O_2 could bind at the site used during amine catalysis. Recent mutagenesis studies, focusing on residues on the C2/C3 side of the TPQ ring, showed a critical role for methionine 634 in the catalytic cycle (*9*). Specifically, the size of the residue at position 634 was shown to correlate linearly with $\log(k_{cat}/K_M)$ for O_2. It therefore appeared that M634 serves a steric role in the oxidative half reaction, which can best be understood in terms of a binding pocket for O_2. Presumably, O_2 accesses this binding pocket from the intersubunit water channel (*15*). It is possible that the enzyme utilizes the same binding pocket in the reaction of Tyr405 with O_2. A recent time-resolved crystallographic study of TPQ genesis in the CAO from *Arthrobacter globiformis* supports this model, as O_2 is shown to react with the precursor tyrosine residue on the methionine-side of the precursor tyrosine ring (*16*).

To test whether M634 might be part of an O_2-binding site during TPQ formation in HPAO, a series of mutations were made at this position and their effects on the TPQ formation reaction monitored. The alanine, leucine, and phenylalanine substitutions were chosen, as these side chains are all hydrophobic and span the range of volumes examined in the previous study of catalysis by these mutants (Table 1) (*9*). It is shown here that replacing methionine with phenylalanine, a side chain of nearly equal volume, has almost no effect on the rate of TPQ formation. Substituting the somewhat smaller leucine side chain has a more pronounced effect on the rate of TPQ formation ($k_{(TPQ)} = 0.042$ min^{-1}), while the very small alanine mutant forms TPQ 2 orders

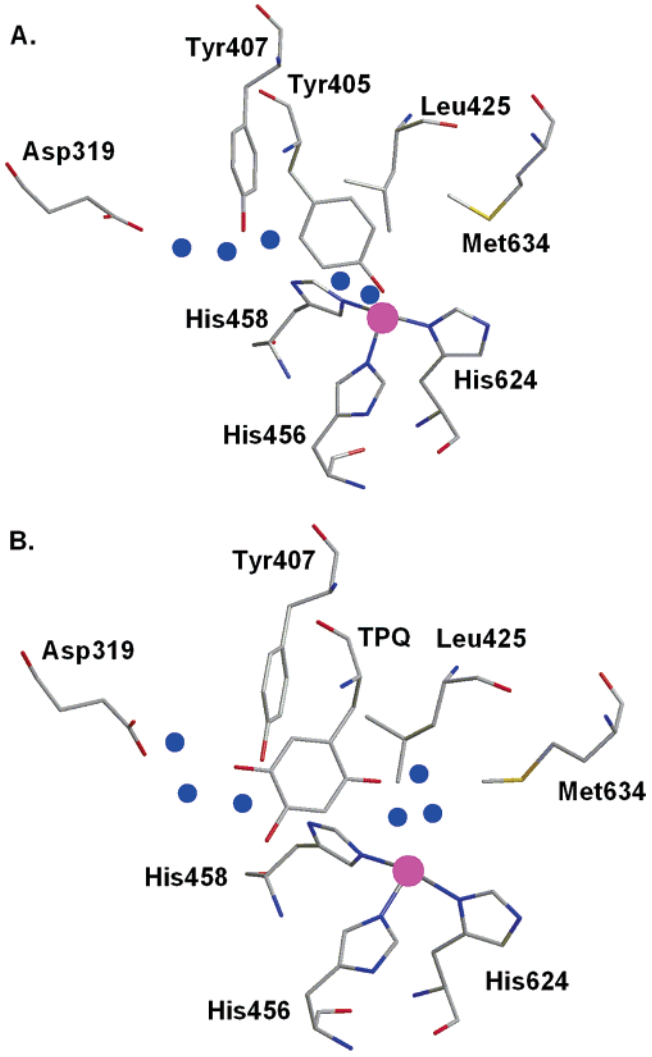

FIGURE 7: (A) Active site structure of Zn(II)/Tyr405 form of HPAO (*14*); (B) active site structure of mature HPAO.

of magnitude more slowly than WT-HPAO. For both M634F and M634L as with WT, an intermediate with a λ_{max} of ca. 350 nm precedes appearance of the cofactor. In the case of M634A, the spectral peak that appears immediately upon oxygenation of the Cu(II)-bound apoprotein is red-shifted and accumulates slowly, over the first ~120 (Figure 5A) rather than 4−5 min (WT-HPAO) of the reaction (*5*). Because the overall absorbance changes are small, occurring over several hours with concomitant increases in the absorbance baseline, it was impossible to quantify the time course of the growth and decay of this species. In particular, isosbestic behavior between this peak and the product TPQ could not be documented. An O_2-dependent peak with similar spectral and temporal characteristics was previously observed for the H624C mutant. By analogy with the wild-type case, the peak was tentatively attributed to an O_2-dependent intermediate (*5*). H624 is a ligand to Cu(II) through its imidazole-ϵ nitrogen. If substitution of a Cu(II) ligand affects the absorbance of an O_2-dependent intermediate, this implies that Cu(II) contributes electronically to the absorbing species and supports the conclusion that the absorbance is due to LMCT. The fact that the M634A mutation effects similar changes in the λ_{max} and time course of the analogous peak could similarly suggest some contribution of M634 to the intermediate's formation and electronic character.

Scheme 4: Two- and Three-Step Mechanisms for the Initial Reaction of Tyr405 with O_2

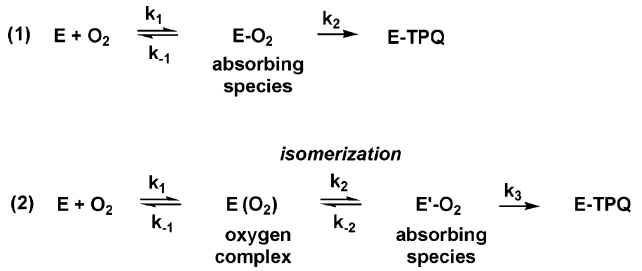

One particularly vexing question has been whether O_2 binding and intermediate formation occur kinetically in a single or separate step(s). A standard means of determining the number of steps in a single-turnover process involving a single substrate is to measure the rate of substrate depletion as a function of [S] (*17*). This was carried out previously in a study of the O_2-dependence of TPQ formation, using an O_2 electrode in a reaction chamber that was not strictly sealed to air (*6*, *7*). However, because the TPQ formation reaction is relatively slow ($t_{1/2}$ = 12 min at 25 °C, pH 7) and because the amount of O_2 consumed in the single-turnover process is low, the background rates in these measurements were very high relative to the actual signal. These data were therefore remeasured using a custom-made, rigorously gastight reaction chamber. While the previous data had shown an approximately linear relationship between $k(O_2)$ and $[O_2]$, data remeasured in the sealed chamber display a hyperbolic curvature (Figure 3). These data were fit to the hyperbolic Michaelis−Menten equation. The value of $[O_2]$ at half the maximum of the curve height, a K_M(effective) for the slow reaction of the enzyme with the first molecule of O_2, is 216 ± 45 μM, which is similar to the K_M(effective) measured by following TPQ formation optically at 480 nm (233 ± 35 μM). The origin of the ca. 2-fold difference in k_{cat} at saturating O_2 is not well-understood. This is not due to the fact that two molecules of O_2 are consumed per TPQ, since this feature is lost when the raw data are fitted to single exponentials for either O_2 depletion or TPQ formation. The most likely explanation is that the microscopic steps that contribute to $k(O_2)$ are different from those in k(TPQ); that is, O_2 will be sequestered within the protein prior to the initiation of TPQ production (see below). Since the data for TPQ production were collected earlier using a different preparation of enzyme precursor (6), it was also possible that the observed differences reflect alterations in enzyme preparations; an argument against this possibility is the excellent agreement among rate constants collected by many different investigators under the standard conditions of pH 7, 25 °C.

Given the evidence that the intermediate is Cu(II)−tyrosinate (and not the further downstream Cu(II)−aryl-peroxide), the initial reaction between enzyme and O_2 could occur in one of two general ways (Scheme 4). Tyr405 and O_2 could collide and react directly to form the intermediate, which then decays in a rate-determining step to yield TPQ (reaction 1). Alternatively, the reaction with O_2 could occur in a two-step process, in which Tyr405 and O_2 form an initial collision complex that undergoes a second isomerization step to form the 350 nm intermediate. This subsequently breaks

down in the rate-determining step to produce TPQ (via k_3 in reaction 2).

We attribute the hyperbolic curves in Figure 3 to saturation in the initially formed enzyme/O_2 collision complex. In the context of the spectroscopic model, the initial intermediate would contain O_2, but the Tyr precursor would remain off the Cu(II). Only upon isomerization of this species would the 350 nm intermediate form, generating TPQ in a subsequent slow step. The new data presented in this manuscript provide support for reaction 2 in Scheme 4. Both spectroscopic and kinetic data point toward a mechanism in which relatively weak O_2 binding near M634 promotes a conformation change that places Tyr405 in close proximity to the Cu(II). The detailed basis for this local structural change is currently unknown. However, previously observed structural differences between precursor and mature forms of HPAO, with regard to the side-chain positions of the amino acids that constitute the putative binding pocket in HPAO, focus attention on this region of the active site as the origin of the O_2-initiated LMCT complex (*16*).

Protein Structural Basis for Cofactor Biogenesis versus Amine Oxidation. As noted previously, the copper amine oxidases are multifunctional proteins that use a single protein fold to catalyze the production of the quino-cofactor and subsequent catalytic reaction. An overlay of structures for the inactive, zinc-containing precursor form of HPAO and the mature enzyme has indicated very limited changes in the positions of amino acid side chains. The only significant differences have been found to reside (i) at tyrosine 405, which moves off the active site metal as it is transformed to TPQ and (ii) in the relationship of methionine 634 and leucine 425 to one another. The finding that Met634 and Leu425 are closer together in the precursor than mature protein led initially to the proposal of different sites of interaction for O_2 in the two enzyme forms (Figure 7B). However, the data presented herein (Table 1 and Figure 6) indicate an almost identical response of O_2 reactivity to mutations at Met634, which leads to the conclusion of very similar sites of O_2 binding during biogenesis and catalysis in HPAO.

This finding narrows even further the protein structural differences that support cofactor production versus catalytic turnover, pointing toward the conformation of residue 405 as a major determinant of chemical reactivity: when Tyr 405 points toward the active site copper, the protein is positioned for monooxygenation, and when it is processed and rotated off of the copper, the protein enters into cycles of reduction by exogenous amines and oxidation by O_2. One feature of the opposing reactivities is their rate differences, with biogenesis occurring at ca. 10^{-3} times the rate of catalysis, implying greater evolutionary constraints on catalytic efficiency than cofactor production. This is reasonable in that formation of TPQ must occur only once and is consistent with relatively low rates of biogenesis of other cofactors (*8, 17*). Most significantly, perhaps, the properties of the CAOs indicate the remarkable plasticity of protein structures in which modest changes in the position of a single side chain can lead to dramatic changes in chemical reactivity.

REFERENCES

1. Mure, M., Mills, S. A., and Klinman, J. P. (2002) Catalytic mechanism of the topa quinone containing copper amine oxidases, *Biochemistry 41*, 9269−9278.
2. Janes, S. M., Mu, D., Wemmer, D., Smith, A. J., Kaur, S., Maltby, D., Burlingame, A. L., and Klinman, J. P. (1990) A new redox cofactor in eukaryotic enzymes−6-hydroxydopa at the active-site of bovine serum amine oxidase, *Science 248*, 981−987.
3. Cai, D. Y., Williams, N. K., and Klinman, J. P. (1997) Effect of metal on 2,4,5-trihydroxyphenylalanine (topa) quinone biogenesis in the *Hansenula polymorpha* copper amine oxidase, *J. Biol. Chem. 272*, 19277−19281.
4. Mu, D., Janes, S. M., Smith, A. J., Brown, D. E., Dooley, D. M., and Klinman, J. P. (1992) Tyrosine codon corresponds to topa quinone at the active-site of copper amine oxidases, *J. Biol. Chem. 267*, 7979−7982.
5. Dove, J. E., Schwartz, B., Williams, N. K., and Klinman, J. P. (2000) Investigation of spectroscopic intermediates during copper-binding and TPQ formation in wild-type and active-site mutants of a copper-containing amine oxidase from yeast, *Biochemistry 39*, 3690−3698.
6. Schwartz, B., Dove, J. E., and Klinman, J. P. (2000) Kinetic analysis of oxygen utilization during cofactor biogenesis in a copper-containing amine oxidase from yeast, *Biochemistry 39*, 3699−3707.
7. Schwartz, B., Olgin, A. K., and Klinman, J. P. (2001) The role of copper in topa quinone biogenesis and catalysis, as probed by azide inhibition of a copper amine oxidase from yeast, *Biochemistry 40*, 2954−2963.
8. Ruggiero, C. E., and Dooley, D. M. (1999) Stoichiometry of the topa quinone biogenesis reaction in copper amine oxidases, *Biochemistry 38*, 2892−2898.
9. Goto, Y., and Klinman, J. P. (2002) Binding of dioxygen to non-metal sites in proteins: exploration of the importance of binding site size versus hydrophobicity in the copper amine oxidase from *Hansenula polymorpha*, *Biochemistry 41*, 13637−13643.
10. Samuels, N. M., and Klinman, J. P. (2005) Manuscript submitted.
11. Yellow Springs Instruments Co., YSI Model 5300 Biological Oxygen Monitor Instruction Manual, Yellow Springs, OH.
12. Su, Q. J., and Klinman, J. P. (1998) Probing the mechanism of proton coupled electron transfer to dioxygen: the oxidative half-reaction of bovine serum amine oxidase, *Biochemistry 37*, 12513−12525.
13. Chen, P., Bell, J., Eipper, B. A., and Solomon, E. I. (2004) Oxygen activation by the noncoupled binuclear copper site in peptidylglycine alpha-hydroxylating monooxygenase. Spectroscopic definition of the resting sites and the putative Cu-M(II)-OOH intermediate, *Biochemistry 43*, 5735−5747.
14. Chen, Z. W., Schwartz, B., Williams, N. K., Li, R. B., Klinman, J. P., and Mathews, F. S. (2000) Crystal structure at 2.5 Å resolution of zinc-substituted copper amine oxidase of *Hansenula polymorpha* expressed in *Escherichia coli*, *Biochemistry 39*, 9709−9717.
15. Li, R. B., Klinman, J. P., and Mathews, F. S. (1998) Copper amine oxidase from *Hansenula polymorpha*: the crystal structure determined at 2.4 Å resolution reveals the active conformation, *Structure 6*, 293−307.
16. Kim, M., Okajima, T., Kishishita, S., Yoshimura, M., Kawamori, A., Tanizawa, K., and Yamaguchi, H. (2002) Copper amine oxidase from *Hansenula polymorpha*: the crystal structure determined at 2.4 Å resolution reveals the active conformation, *Nat. Struct. Biol. 9*, 591−596.
17. Matsuzaki, R., Suzuki, S., Yamaguchi, K., Fukui, T., and Tanizawa, K. (1995) Spectroscopic studies on the mechanism of the topa quinone generation in bacterial monoamine oxidase, *Biochemistry 34*, 4524−4530.

BI0504759